

# Gaseous Nanobubbles - Surface Nanopatterning Elements

P. Janda\* and H. Tarabkova\*

\* J. Heyrovsky Institute of Physical Chemistry ASCR, v.v.i.  
Dolejskova 3, CZ 182 23 Prague 8, Czech Republic, pavel.janda@jh-inst.cas.cz

## ABSTRACT

Nanobubble assisted nanopatterning of solid surfaces has been studied on hydrophobic surface immersed in de-ionized water. Mild ( $<10$  kPa) pressure drop applied on solid liquid interface at room temperature caused nanobubble imprint formation on the surface of polymeric film within exposition time of seconds. Imprints in solid indicating surface rearrangement taking place at nanobubble positions were examined by in situ and ex situ atomic force microscopy. Surface rearrangement correlates with material properties of solid such as Young Modulus etc. of solid exposed to nanobubbles.

**Keywords:** nanobubbles, gaseous nanodomains, surface nanopatterning, quasiperiodic arrangement

## 1 INTRODUCTION

Gaseous nanodomains – nanobubbles and nanopancakes (Fig. 1) - appearing at solid-liquid interface represent a challenging topic intensively studied last few years. Parker, Claesson and Attard [1] first pointed to long range ( $\sim 10^2$  nm) attractive forces appearing between two adjacent planar solid hydrophobic surfaces immersed in water and ascribed them to sub-micro bubbles bridging both surfaces. Though this assumption was later confirmed by in-situ AFM images of nanobubbles on immersed solid surfaces, the nanobubble concept was still mostly refused due to the absence of plausible explanation of their existence. Since then, gaseous nanodomains were confirmed as a real phenomenon. While some promising models such as Knudsen gas behavior [2] appeared, compact and plausible physical explanation of their stability, which seemingly violates the Young-Laplace law, as well as the clarification of other anomalies of nanobubble existence, is still missing.

Our work is focused on interactions which gaseous nanodomains exhibit at solid/liquid interface and their implications for altering surface nanomorphology respectively.

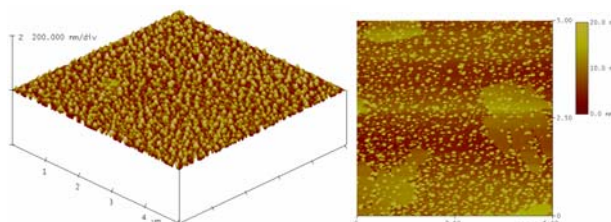


Figure 1: In-situ AFM (tapping) image of gaseous nanodomains: Nanobubbles covering surface of polystyrene film (left) and nanopancakes observed on basal plane HOPG (right), both immersed in de-ionized water.

## 2 NANOBUDDLE INTERACTION WITH SOLID SURFACE

Forces at nanobubble perimeter have been already found to be responsible for surface cleaning – nanobubbles cause removal of deposits and adsorbates respectively [3][4], while nanomorphology changes of solid surface were so far explained as a consequence of ion [5] rather than nanobubble interaction. Bhushan et al [6] reported on nanoindents formed in polystyrene film on sites occupied by nanobubbles upon its immersion in water.

As we have shown, nanobubbles can play a protective role preventing adsorption of surface active compounds [7].

Besides that however, we have found, that forces at the nanobubble ternary interface are capable to rearrange significantly the surface of solids (Fig. 2).

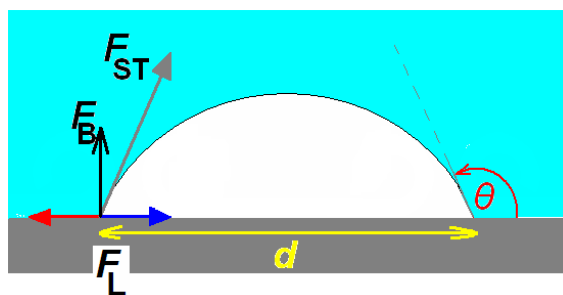


Figure 2: Simplified scheme of forces acting at the bubble ternary interface of diameter  $d$  and contact angle  $\theta$ : Force expressing the surface (gas/liquid) tension ( $F_{ST}$ ), its lateral component ( $F_L$ ) adding to nanobubble pinning [8] and buoyancy force ( $F_B$ ) adding to bubble lifting capability.

For the first time we have noticed the nanobubble-assisted room temperature non-oxidative exfoliation of graphene sheets on basal planes of highly ordered pyrolytic graphite (HOPG) immersed in de-ionized water[9].

Remarkable nanobubble-assisted nanopatterning, which we have observed on polystyrene [10] and on PTFE layered surfaces (Figures 4, 5) respectively, led us to consider forces existing at ternary nanobubble interface (Fig. 2): The lateral force component  $F_L$  corresponds to

$$F_L = F_{ST} \cos(180 - \theta) \quad (1)$$

with

$$F_{ST} = \gamma \pi d \quad (2)$$

where  $\gamma$  represents the surface tension (for air-water  $\gamma \sim 70$  mN/m) acting at the nanobubble perimeter  $\pi d$ . The tension and buoyancy forces appear to compose shrinking and lifting effects on the solid surface at the contact line of expanding nanobubble, especially when the interface pinning is considered [8].

We can elucidate in the simplified approach (in case of polystyrene), that the tensile stress induced by interfacial forces at nanobubble contact line exceeds at least  $\sigma > 10^2$  MPa.

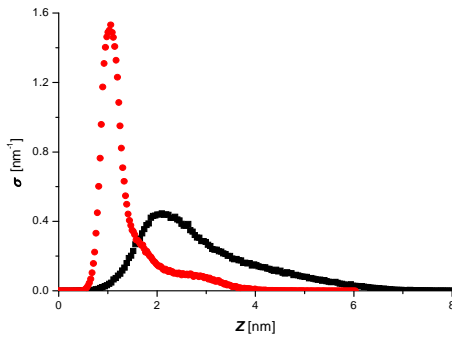


Figure 3: Height ( $Z$ ) density distribution ( $\sigma$ ) of nanopatterns formed on basal plane HOPG (circles) and polystyrene surface (squares)

While height distribution of nanopatterning on polystyrene surface shows broad maximum at 2-3 nm with distribution reaching above 5 nm, HOPG shows narrow curve with maximum at 1-2 nm, reaching above 3 nm (Fig. 3). The narrow distribution indicates well defined mechanism of pattern formation with lower fluctuation of material properties as can be expected at multilayer highly ordered graphene surface. Graphene tearing followed by spontaneous scrolling and buckling, driven by interlayer van der Waals forces, is expected to yield compact nanoparticle dimensional distribution. In case of tearing multilayer graphene leaves however, we can expect that exfoliation takes place preferably on surface imperfections

and defects, having strength substantially lower, than for single layer (defect free) graphene.

It should be emphasized, that the nanobubble-assisted nanopatterning was found not be related to any elevated-energy process including implosive cavitation etc. Instead, it proceeds at very mild conditions (de-ionized water, room temperature, absence of any chemical reaction). It appears to be triggered by relatively short ( $\sim 1$  sec) mild ( $< 10$  kPa) pressure drop applied on the solid liquid interface. Within this exposition time interval single-step surface nanopatterning takes place on immersed area exposed to nanobubbles.

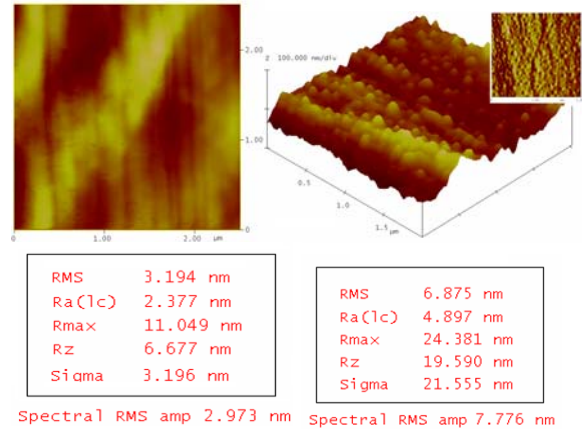


Figure 4: Ex-situ AFM image (tapping, height) of layered PTFE before (left) and after exposure to nanobubbles in de-ionized water (right). Corresponding roughness analysis tables (below) show significant increase of surface nanoroughness

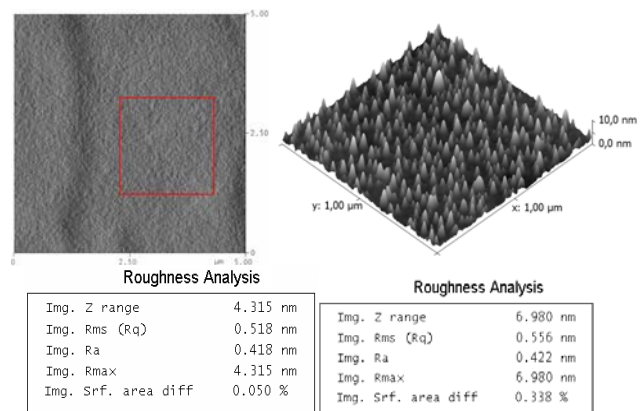


Figure 5: AFM (tapping) image of polystyrene film before (left) and after (right) exposition to nanobubbles in deionized water upon mild pressure drop ( $\sim 5$  kPa), at room temperature ( $20^\circ\text{C}$ ). Red square indicates zoomed area shown on the 3D image. The increase of surface roughness is illustrated by roughness analysis tables below each image.

Besides random nanopatterning shown in Figs 4 and 5, quasi-periodic net-like nanopattern arrangement with high degree of order can be formed under specific conditions on polymeric matrix (Fig. 6).

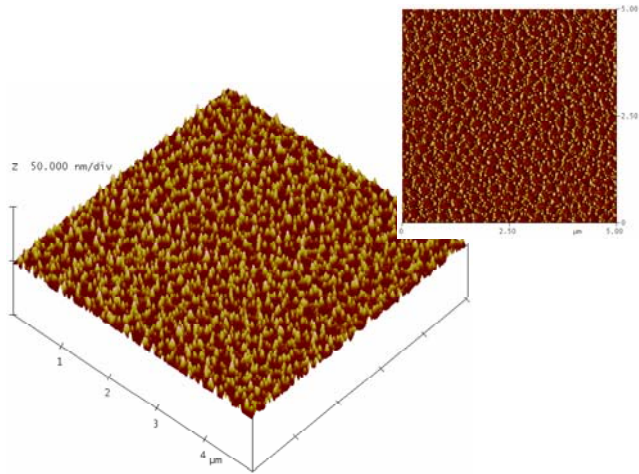


Figure 6: AFM (tapping, height) image of net nanopattern formed upon nanobubble exposition on polystyrene immersed in de-ionized water.

According to our understanding, the net nanopattern appears to represent imprint of surface-confined 2D nanofoam, indicating existence of relatively large areas of 2D close-packed nanobubble aggregates with narrow nanobubble size distribution, localized at solid/liquid interface on immersed solid surface. From that point the nanostructure can be considered as so called “wet” nanofoam. Nanobubbles can fulfill nanofoam stabilizing function, similar to micelles and other nanoparticles, which are also known to stabilize foams. Thus, the nanofoam can be formed as an aggregate of larger sub-micro bubbles combined with nanobubbles filling the interbubble space.

Close-packed arrangement can be formed by single layer 2D nanofoam, while larger spacing can be assigned to two-layer 2D nanofoam, where nanobubbles in one layer are positioned in spacing of another one. Bottom layer is imprinted in polystyrene surface.

While the exact mechanism of net-patterning is still under investigation, two models appear to be more plausible:

Neighbouring nanobubbles upon expansion can compress surface polymeric film between them, which is then lifted, while the rest of the surface (covered by nanobubble) remains intact (Fig. 7).

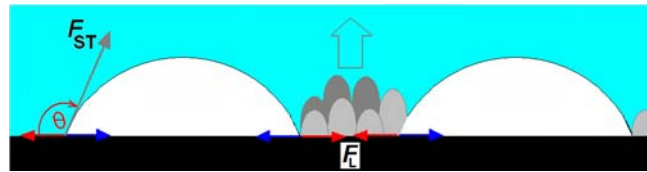


Figure 7: Squeezing and lifting polymeric film between expanding neighbour nanobubbles forms net-like nanopattern.

Second model is based on the fact that bubble aggregates are known to be often formed by bubbles of different size distributions. Larger sub-micro bubbles play – compared to significantly smaller nanobubbles – protective role, while orders of magnitude smaller nanobubbles with higher interfacial forces – cause surface nanopatterning. This model is supported by protective role of large sub-micro and micro-bubbles observed e.g. on AFM images of nanopatterned HOPG (Fig. 8) and polystyrene [10].

This effect may indicate the nanobubble interfacial force magnitude declines towards larger bubble dimensions. Besides surface nanopatterning, the imaging nanobubbles by their imprints in polymeric matrix was considered (“nanobubblegraphy”[10]).

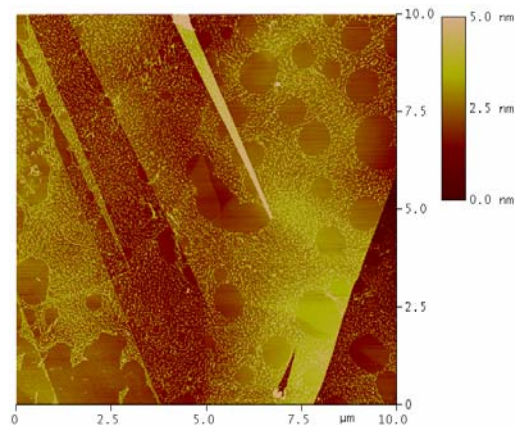


Figure 8: AFM image illustrating protective role of large (micro) bubbles (hollow rounded areas) compared to nanopatterning by nanobubbles (nanoroughened surface areas between them).

In all cases the extent of surface rearrangement was found to show strong correlation with surface hydrophobicity and material properties of solid surface respectively, characterized e.g. by Young Modulus.

### 3 ACKNOWLEDGEMENT

Acknowledged project support: GACR P208/12/2429

## REFERENCES

- [1] J. L. Parker, P. M. Claesson, P. Attard: Bubbles, cavities, and the long-ranged attraction between hydrophobic surfaces. *J. Phys. Chem.* 98, 8468, 1994.
- [2] J. R. T. Seddon, H. J.W. Zandvliet, D. Lohse: Knudsen Gas Provides Nanobubble Stability. *Phys. Rev. Lett.* 107, 116101, 2011.
- [3] Z. Wu, H. Chen, Y. Dong, H. Mao, J. Sun, S. Chen, V. S.J. Craig: Cleaning using nanobubbles: Defouling by electrochemical generation of bubbles, *J. Colloid Interface Sci.* 328, 10, 2008.
- [4] G. Liu, Z. Wu, V. S. J. Craig: Cleaning of Protein-Coated Surfaces Using Nanobubbles: An Investigation Using a Quartz Crystal Microbalance, *J. Phys. Chem. C* 112, 16748, 2008.
- [5] I. Siretanu, J. P. Chapel, C. Drummond: Water Ions Induced Nanostructuring of Hydrophobic Polymer Surfaces, *ACS Nano* 5, 2939, 2011.
- [6] Y. Wang, B. Bhushan, X. Zhao: Nanoindents produced by nanobubbles on ultrathin polystyrene films in water, *Nanotechnology* 20, 045301, 2009.
- [7] V. Kolivoska, M. Gal, M. Hromadová, S. Lachmanova, H. Tarabkova, P. Janda, L. Pospisil, A. Morovska Turonova: Bovine serum albumin film as a template for controlled nanopancake and nanobubble formation: In situ atomic force microscopy and nanolithography study, *Colloids Surf.,B* 94, 213 2012.
- [8] Y. Liu, X. Zhang: Nanobubble stability induced by contact line pinning, *J. Chem. Phys.*, 138, 014706, 2013.
- [9] P. Janda, O. Frank, Z. Bastl, M. Klementova, H. Tarabkova, L. Kavan: Nanobubble-assisted formation of carbon nanostructures on basal plane highly ordered pyrolytic graphite exposed to aqueous media, *Nanotechnology* 21, 095707, 2010.
- [10] H. Tarabkova, P. Janda: Nanobubble assisted nanopatterning utilized for ex situ identification of surface nanobubbles, *J. Phys.: Condens. Matter* 25, 184001, 2013.